PHYSICAL REVIEW A, VOLUME 64, 063401

Interrelation between high-order harmonic generation and above-threshold ionization

Panming Fu, Bingbing Wang, Xiaofeng Li, and Lianghui Gao
Laboratory of Optical Physics, Institute of Physics and Center for Condensed Matter Physics, Chinese Academy of Sciences, Beijing 100080, China

(Received 4 June 2001; published 9 November 2001)

We study the interrelation between high-order harmonic generation (HHG) and above-threshold ionization (ATI) in the frequency domain. HHG can be described simply as an ATI followed by laser assisted recombination (LAR). The plateau reflects mainly the characteristics of LAR. We also study the correspondence between frequency-domain and time-domain pictures of HHG.

DOI: 10.1103/PhysRevA.64.063401 PACS number(s): 42.50.Hz, 42.65.Ky, 32.80.Rm

I. INTRODUCTION

There is much current interest in the multiphoton effects occurring when atoms are exposed to high-intensity laser fields. Above-threshold ionization (ATI) and high-order harmonic generation (HHG) have been investigated extensively. In the ATI process, atoms absorb more photons than the minimum number of photons required by energy conservation, resulting in distribution of the photoelectrons among the ATI channels. Atoms can also emit very high harmonics when interacting with intense laser fields. The HHG is characterized by a rapid drop at low orders, followed by a broad plateau where all the harmonics have the same strength, and a sharp cutoff at frequency $E_B+3.2u_p$, where E_B and u_p are the atomic ionization potential and the electron ponderomotive energy in the laser field, respectively. Since the relationship between HHG and ATI is fundamental to the understanding of strong-field laser-atom interactions, attempts have been made to investigate the relation between these two multiphoton effects [1–3]. Eberly *et al.* [1] suggested a simple relation between them by comparing the corresponding ATI and HHG spectra. Becker *et al.* [2] established a general formal relation between ionization and HHG. Kuchiev and Ostrovsky [3] present HHG as an ATI followed by continuum electron propagation in a laser field and subsequent stimulated recombination back into the initial state.

The interpretation of HHG processes is usually given by a three-step semiclassical description [4]. In this model, the electron first tunnels from the atomic ground state through the barrier formed by the Coulomb potential and the laser field. Its subsequent motion can be treated classically and consists of free oscillations driven by the laser field. If the electron return to the vicinity of the nucleus, it may recombine and emit a harmonic photon. The three-step semiclassical model gives very important insight into the physics of the cutoff law. However, this model does not relate to the ATI process because the discrete ATI channels do not appear within the classical framework. Moreover, it cannot explain the existence and origin of the plateau. More sophisticated approaches, which include the effects of quantum tunneling, quantum diffusion, and interference, have been developed lately [5,6].

The three-step model considers the temporal evolution of the electronic wave packet under the interaction of a light field. It can be regarded as the time-domain description of HHG. We may also study HHG in the frequency domain. From this viewpoint, HHG involves a ionization of the electron from the ground state after absorbing photons from the laser field, followed by a return of the electron to the ground state with harmonic photon emission. Shore and Knight [7] have studied the generation of optical harmonics from the dressed photoionization continuum. On the other hand, we have presented a frequency-domain description of HHG through quantizing the electromagnetic field [8]. In this paper we will show that, from this viewpoint, HHG can be described simply as an ATI followed by laser assisted recombination (LAR). Moreover, the plateau in the harmonics spectrum reflects mainly the characteristics of LAR.

It should be noted that, although we quantize the electromagnetic field in our QED treatment of HHG, it does not mean that quantized-field effects are important in multiphoton processes. As is well known, effects that are due to field quantization are of relative order $1/n$, with n the number of field quanta of the relevant mode [9]. Therefore, the quantized-field effects are extremely small in HHG. Actually, we will show that the Landau-Dykhne formula which represents the quantum-mechanical formulation of the three-step model can be derived from our theory. We adopt the QED approach here because it provides a means to understand HHG in the frequency domain, and from this viewpoint the connection between ATI and HHG becomes obvious.

This paper is organized as follows. In Sec. II we study the interrelation between HHG and ATI in the frequency domain. HHG can be described as an ATI followed by LAR. The plateau reflects mainly the characteristics of LAR. Numerical results also indicate that low ATI channels are essential for characterizing the HHG spectrum. In Sec. III we establish the correspondence between frequency-domain and time-domain pictures of HHG. We show that, through purposely introducing time variables into the time-independent transition matrix, the Landau-Dykhne formula which represents the quantum-mechanical formulation of the three-step model can be derived. Section IV is the discussion and conclusion.

II. INTERRELATION BETWEEN HHG AND ATI

We consider a quantized single-mode laser field of frequency ω with wave vector $\mathbf{k}$ and a high-harmonic photon mode of frequency ω' with wave vector $\mathbf{k}'$. The Hamiltonian of the atom-radiation system is

$$H = H_0 + U(\mathbf{r}) + V + V', \tag{1}$$

where

$$H_0 = [(-i\boldsymbol{\nabla})^2/2m_e] + \omega N_a + \omega' N_a' \tag{2}$$

is the noninteraction part of the Hamiltonian. Here, $N_a = (a^\dagger a + a a^\dagger)/2$ and $N_a' = (a'^\dagger a' + a' a'^\dagger)/2$ are photon number operators of the laser and the harmonic photon mode, respectively, with a and a' being the annihilation operators and $a^\dagger$ and $a'^\dagger$ the creation operators. $U(\mathbf{r})$ is the atomic binding potential;

$$V = -(e/m_e)\mathbf{A}(\mathbf{r})\cdot(-i\boldsymbol{\nabla}) + (e^2/2m_e)\mathbf{A}^2(\mathbf{r}), \tag{3}$$

$$V' = -(e/m_e)\mathbf{A}'(\mathbf{r})\cdot(-i\boldsymbol{\nabla}) + (e^2/m_e)\mathbf{A}(\mathbf{r})\cdot\mathbf{A}'(\mathbf{r}) \tag{4}$$

are the interaction between the electron and the laser field and the harmonic mode, respectively. Here, the vector potentials are $\mathbf{A}(\mathbf{r}) = g[\hat{\boldsymbol{\epsilon}} a \exp(i\mathbf{k}\cdot\mathbf{r}) + \text{c.c.}]$ and $\mathbf{A}'(\mathbf{r}) = g'[\hat{\boldsymbol{\epsilon}}' a' \exp(i\mathbf{k}'\cdot\mathbf{r}) + \text{c.c.}]$ for the laser and harmonic mode, respectively; $g = (2\omega V_\gamma)^{-1/2}$, $g' = (2\omega' V_\gamma')^{-1/2}$; V_γ and V_γ' are the normalization volumes of the photon modes; $\hat{\boldsymbol{\epsilon}} = \hat{\boldsymbol{\epsilon}}_x \cos(\xi/2) + i\hat{\boldsymbol{\epsilon}}_y \sin(\xi/2)$ and $\hat{\boldsymbol{\epsilon}}'$ are the polarization vectors of the laser mode and the harmonic mode respectively. We neglect the $\mathbf{A}'^2$ term because of its weak strength.

The initial and final states of HHG are taken as $|\psi_i\rangle \equiv |\Phi_i(\mathbf{r}), n_i, 0\rangle \equiv \Phi_i(\mathbf{r}) \otimes |n_i\rangle \otimes |0\rangle'$ and $|\psi_f\rangle \equiv |\Phi_i(\mathbf{r}), n_f, 1\rangle \equiv \Phi_i(\mathbf{r}) \otimes |n_f\rangle \otimes |1\rangle'$, which are the eigenstates of the Hamiltonian $H_0 + U(\mathbf{r})$ with eigenenergies $E_i = -E_B + (n_i + \frac{1}{2})\omega + \frac{1}{2}\omega'$ and $E_f = -E_B + (n_f + \frac{1}{2})\omega + \frac{3}{2}\omega'$, respectively, where $\Phi_i(\mathbf{r})$ is the ground-state wave function of the atomic electron with binding energy E_B, $|n_i\rangle$ and $|n_f\rangle$ are the Fock states of the laser mode with photon numbers n_i and n_f, and $|0\rangle'$ and $|1\rangle'$ are those of the harmonic mode. Energy is conserved throughout the interaction, resulting in $\omega' = q\omega$ with $q = n_i - n_f$. Then, the transition matrix element for the qth order harmonic is [8]

$$T^{(q)} = i\pi \sum_{\mathbf{P}n} [\langle \psi_f | V' | \Psi^0_{\mathbf{P}n,0} \rangle \langle \Psi^0_{\mathbf{P}n,0} | V | \psi_i \rangle \delta(E_i - E(\mathbf{P}n, 0)) + \langle \psi_f | V | \Psi^0_{\mathbf{P}n,1} \rangle \langle \Psi^0_{\mathbf{P}n,1} | V' | \psi_i \rangle \delta(E_i - E(\mathbf{P}n, 1))]. \tag{5}$$

The differential rate of emission of a harmonic photon is obtained by squaring the transition matrix element, i.e.,

$$\frac{dw}{d\Omega} = \frac{V_r}{(2\pi)^2} \omega'^2 |T_{fi}|^2. \tag{6}$$

In deriving Eq. (5), the long-wavelength approximation is used. Here, $\Psi^0_{\mathbf{P}n,n'} = \Psi^0_{\mathbf{P}n} |n'\rangle$ is the direct product of a quantized Volkov state $\Psi^0_{\mathbf{P}n}$ and a Fock state $|n'\rangle$ of the harmonic mode with eigenenergy $E(\mathbf{P}n, n') = E^0_{\mathbf{P}n} + (n' + \frac{1}{2})\omega'$. The quantized Volkov state [10]

$$\Psi^0_{\mathbf{P}n} = V_e^{-1/2} \sum_{j=-n}^{\infty} \exp\{i[\mathbf{P} + (u_p - j)\mathbf{k}]\cdot\mathbf{r}\} \mathcal{J}_j(\zeta, \eta, \phi_{\hat{\xi}})^* \exp(-ij\phi_{\hat{\xi}}) |n + j\rangle, \tag{7}$$

with corresponding energy eigenvalues $E^0_{\mathbf{P}n} = (\mathbf{P}^2/2m_e) + (n + \frac{1}{2} + u_p)\omega$, is the eigenstate of the electron-laser-mode subsystem with Hamiltonian $H_0 + V$. Here, $u_p = e^2\Lambda^2/m_e\omega$ is the ponderomotive energy in units of the photon energy of the laser. The limit $g\sqrt{n} \to \Lambda$ $(g \to 0,\ n \to \infty)$ is the half amplitude of the classical field. The generalized Bessel functions $\mathcal{J}_j$ are defined in terms of ordinary Bessel functions as

$$\mathcal{J}_j(\zeta, \eta, \phi_{\hat{\xi}}) = \sum_{m=-\infty}^{\infty} J_{-j-2m}(\zeta) J_m(\eta) (-1)^j e^{2im\phi_{\hat{\xi}}}, \tag{8}$$

where $\zeta = (2|e|\Lambda/m_e\omega)|\mathbf{P}\cdot\hat{\boldsymbol{\epsilon}}|$, $\eta = (u_p/2)\cos\xi$, and $\phi_{\hat{\xi}} = \tan^{-1}[(P_y/P_x)\tan(\xi/2)](+\pi)$.

Considering the first term in Eq. (5), $\langle \Psi^0_{\mathbf{P}n,0} | V | \psi_i \rangle$ represents the ATI amplitude of the KFR (Keldysh-Faisal-Reiss) model [10,11], where the ground-state electron absorbs $n_i - n$ photons from the laser field and ionizes; whereas $\langle \psi_f | V' | \Psi^0_{\mathbf{P}n,0} \rangle$ represents the amplitude of LAR in which the continuum electron absorbs $n - n_f$ extra photons from the field and returns to the bound state by emitting a single photon of frequency ω'. Now we consider the second term in Eq. (5). $\langle \Psi^0_{\mathbf{P}n,1} | V' | \psi_i \rangle$ represents a process where the ground-state electron absorbs $n_i - n$ photons from the laser field and ionizes. At the same time, a harmonic photon with frequency $(n_i - n_f)\omega$ is emitted. $\langle \psi_f | V | \Psi^0_{\mathbf{P}n,1} \rangle$ represents a process where the continuum electron emits $n_f - n$ photons to the laser field and returns to the bound state. From our calculations, the contribution from the second term can be neglected because it involves many more photons at the first step. Therefore, HHG can be described simply as an ATI followed by LAR.

We consider a hydrogenlike atom ($E_B = 13.6$ eV) irradiated by a linearly polarized Nd:YAG (yttrium aluminum garnet) laser ($\omega = 1.165$ eV) of intensity 1.9×10^{14} W/cm^2. The corresponding parameters are $u_p = 20$ and $E_B/\omega = 11.7$. The ground-state s wave function in the momentum space is assumed to be the Gaussian form $\Phi(|\mathbf{P}|) = (4\pi/\alpha)^{3/4} \exp[-(P^2/2\alpha)]$ with $\alpha = 2m_e E_B$. By neglecting the second term in Eq. (5), we express Eq. (5) as $T^{(q)} \simeq \Sigma_k T_k^{(q)}$. Here,

$$T_k^{(q)} = i\pi \sum_{\mathbf{P}} \langle \psi_f | V' | \Psi^0_{\mathbf{P}n,0} \rangle \langle \Psi^0_{\mathbf{P}n,0} | V | \psi_i \rangle \delta(E_i - E(\mathbf{P}n, 0)) \tag{9}$$

with $n = n_i - j_0 - k + 1$; j_0 is the minimum number of photons the atoms need to absorb to achieve ionization. Due to the ponderomotive shift, we have $j_0 = 32$ for $u_p = 20$ and $E_B/\omega = 11.7$. Physically, $T_k^{(q)}$ corresponds to the contribution from the kth ATI channel. Figure 1 presents the HHG spectra for separate ATI channels, where the solid, dashed, dot-dashed, and dotted curves correspond to $k = 1$, 3, 8, and 50, respectively. For reference, the ATI spectrum is also given in the inset. These spectra reflect the characteristics of LAR

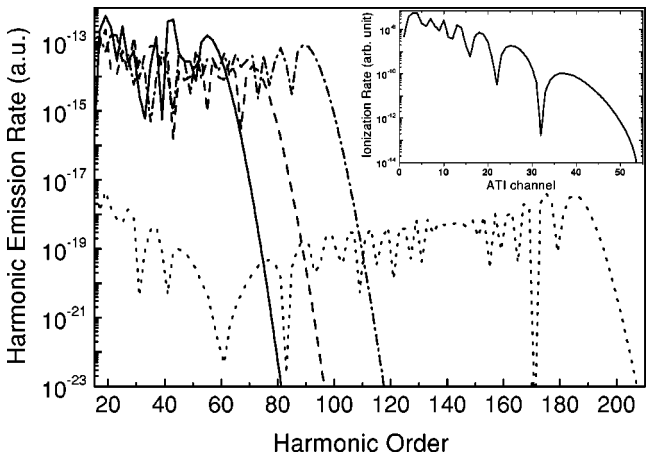

FIG. 1. Harmonic spectra from separate ATI channels with $k=1$ (solid curve), $k=3$ (dashed curve), $k=8$ (dot-dashed curve), and $k=50$ (dotted curve). The corresponding parameters are $u_p=20$ and $E_B/\omega=11.7$. For reference, the ATI spectrum is given in the inset.

when the electrons are in different ATI channels. All spectra exhibit a plateau followed by a clear cutoff, which occurs at $q=55$, 71, 89, and 185 for $k=1$, 3, 8, and 50, respectively. We then present the HHG spectrum when the contributions from all ATI channels are added up coherently (thick solid curve in Fig. 2). The cutoff occurs at the 79th harmonic order. For comparison, we also give the HHG spectrum with a finite number of ATI channels. The thin solid, dashed, dot-dashed, and dotted curves in Fig. 2 present the HHG spectra when we include one ($k=1$), three ($k=1-3$), eight ($k=1-8$) and 50 ($k=1-50$) ATI channels, respectively. These curves indicate that only eight ATI channels are required to characterize the HHG spectrum with correct cutoff. To get further understanding of the role of the low ATI channels, Fig. 3 presents the HHG spectra when the contribution from the first three (thick solid curve), first eight (dashed curve),

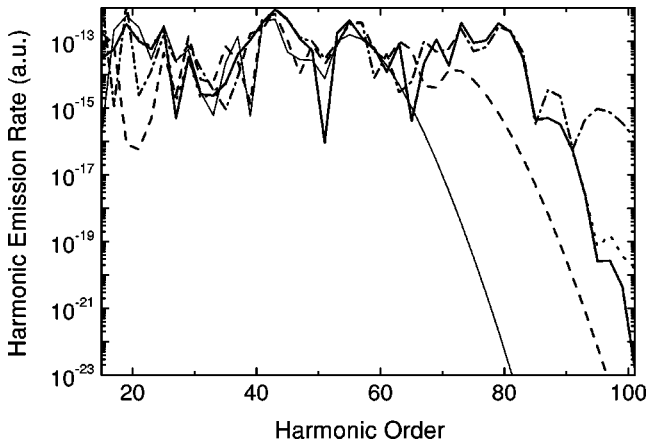

FIG. 2. Harmonic spectrum when the contributions from all ATI channels are added up coherently (thick solid curve). The corresponding parameters are $u_p=20$ and $E_B/\omega=11.7$. Harmonic spectra that include one (thin solid curve), three (dashed curve), eight (dot-dashed curve), and 50 (dotted curve) ATI channels are also presented.

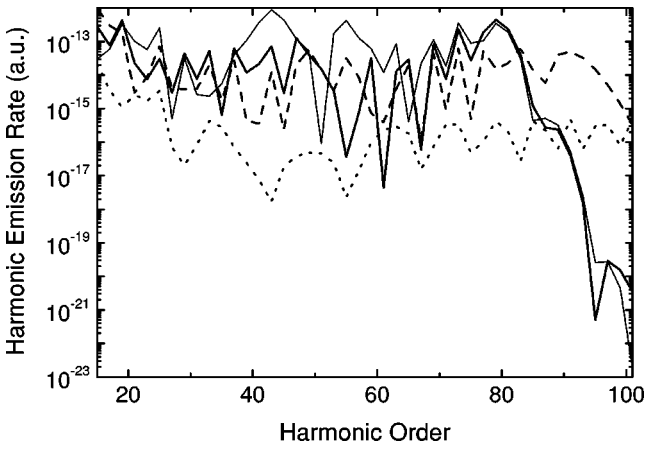

FIG. 3. Harmonic spectra when the contribution from the first three (thick solid curve), first eight (dashed curve), and first 30 (dotted curve) ATI channels are omitted. The thin solid curve presents the harmonic spectrum that includes all ATI channels. The corresponding parameters are $u_p=20$ and $E_B/\omega=11.7$.

and first 30 (dotted curve) ATI channels are omitted. For reference, the HHG spectrum that includes all ATI channels is also given (thin solid curve). When the first three ATI channels are omitted, the HHG spectrum shows a plateau with the correct cutoff frequency. In contrast, the HHG spectrum displays the wrong cutoff frequency if we disregard the first eight ATI channels. Figures 2 and 3 indicate that low ATI channels are essential for characterizing the HHG spectrum. The importance of the low ATI channels for HHG is consistent with semiclassical theory [4]. The canonical (drift) momentum of a free electron moving in a classical field with velocity $\mathbf{v}$ is given by $\mathbf{P}=\mathbf{v}+\mathbf{A}_c(t)$. According to the semiclassical theory, the dominant contribution to HHG comes from electrons that tunnel into the continuum with zero velocity at a time near the peak of the laser field. They correspond to low ATI channels with small values of drift momentum. Our results also indicate that, to obtain a good convergence at the cutoff region, as many as about 50 ATI channels should be added up coherently. According to the semiclassical theory, for a harmonic belonging to the cutoff there is only one electron trajectory that contributes to the generation process. The involvement of more than 50 ATI channels in the cutoff region is attributed to the construction of the single-electron trajectory from the quantized Volkov states, which are stationary eigenstates of the system. Similar results are found when the incident light is elliptically polarized.

III. CORRESPONDENCE BETWEEN FREQUENCY-DOMAIN AND TIME-DOMAIN PICTURES OF HHG

In the frequency-domain picture, HHG involves a transition of an electron from the ground state to a quantized-field Volkov state under the interaction of the laser field followed by a return of the electron to the ground state with harmonic photon emission. The emission of the harmonic photon is described by a time-independent transition matrix. In contrast, the time-domain three-step model considers the tempo-

ral evolution of the electronic wave packet under the interaction of the light field. In order to clarify the intrinsic connection between these two pictures, here we show that, through purposely introducing time variables into the time-independent transition matrix, the Landau-Dykhne formula which represents the quantum-mechanical formulation of the three-step model can be derived.

Considering the first term in Eq. (5), it can be rewritten as

$$T^{(q)}=\sum_{\mathbf{P}n}\langle\psi_f|V'\frac{1}{E_i-(H_0+V+V')+i\epsilon}|\Psi^0_{\mathbf{P}n,0}\rangle \times\langle\Psi^0_{\mathbf{P}n,0}|V|\psi_i\rangle. \tag{10}$$

To introduce time variables into the above equation, we employ the following two identities:

$$\frac{1}{E_i-(H_0+V+V')+i\epsilon} =-i\int_{-\infty}^{t}dt'\exp\{-i[E_i-(H_0+V+V')+i\epsilon](t'-t)\} \tag{11}$$

and

$$\langle\psi_f|V'|\Psi^0_{\mathbf{P}n,0}\rangle\langle\Psi^0_{\mathbf{P}n,0}|V|\psi_i\rangle =\langle\psi_f|U^\dagger(t)V'(t)U(t)|\Psi^0_{\mathbf{P}n,0}\rangle \times\langle\Psi^0_{\mathbf{P}n,0}|U^\dagger(t')V(t')U(t')|\psi_i\rangle. \tag{12}$$

Here $U(t)=\exp(i\omega tN_a)$ is a unitary operator; $V(t')=U(t')VU^\dagger(t')=(e/m_e)\mathbf{A}(t')\cdot[i\boldsymbol{\nabla}+(e/2)\mathbf{A}(t')]$ and $V'(t)=U(t)V'U^\dagger(t)=(e/m_e)\mathbf{A}'\cdot[i\boldsymbol{\nabla}+e\mathbf{A}(t)]$. In the long-wavelength approximation, the time-dependent vector potential is $\mathbf{A}(t)=g[\hat{\boldsymbol{\epsilon}}a\exp(-i\omega t)+\text{c.c.}]$. As pointed out by Becker *et al.* [2], the matrix element $\mathbf{D}(t)$, which is closely related to the ground-state expectation value of the dipole moment, is the Fourier transform of the transition matrix element. With the help of Eqs. (7), (11), and (12), we obtain from Eq. (10)

$$\mathbf{D}^+(t)=\sum_q T^{(q)}\exp(-iq\omega t) =-iV_e^{-1}\left(\frac{e}{m_e}\right)^2 g'\int_{-\infty}^{t}dt'\int d\mathbf{P} \times\langle\Phi_i|[i\boldsymbol{\nabla}+e\mathbf{A}_c(t)]|\mathbf{P}\rangle \times\langle\mathbf{P}|\mathbf{A}_c(t')\cdot\left[i\boldsymbol{\nabla}+\frac{e}{2}\mathbf{A}_c(t')\right]|\Phi_i\rangle \times\exp[-iS(\mathbf{P},t,t')]. \tag{13}$$

Here, $|\mathbf{P}\rangle=\exp(i\mathbf{P}\cdot\mathbf{r})$ represents the electron plane wave of momentum $\mathbf{P}$; $\mathbf{A}_c(t)=\Lambda[\hat{\boldsymbol{\epsilon}}\exp(-i\omega t)+\text{c.c.}]$ is the vector potential of the classical field;

$$S(\mathbf{P},t,t')=\int_{t'}^{t}dt''([\mathbf{P}-\mathbf{A}_c(t'')]^2/2+E_B)$$

is the quasiclassical action. In deriving Eq. (13), the only approximation we made is to replace the Fock states $|n+j\pm1\rangle$ and $|n+j\pm2\rangle$ by $|n+j\rangle$. Similarly, the matrix element $\mathbf{D}^-(t)$ corresponding to the second term in Eq. (5) is

$$\mathbf{D}^-(t)=-iV_e^{-1}\left(\frac{e}{m_e}\right)^2 g'\int_{-\infty}^{t}dt'\int d\mathbf{P} \times\langle\Phi_i|\mathbf{A}_c(t)\cdot\left[i\boldsymbol{\nabla}+\frac{e}{2}\mathbf{A}_c(t)\right]|\mathbf{P}\rangle \times\langle\mathbf{P}|[i\boldsymbol{\nabla}+e\mathbf{A}_c(t')]|\Phi_i\rangle\exp[-iS(\mathbf{P},t,t')]. \tag{14}$$

The total matrix element $\mathbf{D}(t)=\mathbf{D}^+(t)+\mathbf{D}^-(t)$.

Equation (13) is the Landau-Dykhne formula in the $\mathbf{A}\cdot\mathbf{P}$ gauge [12], which represents the quantum-mechanical formulation of the three-step model. Physically, an electron initially in the ground state of an atom makes a transition to the continuum at time t' with the canonical momentum $\mathbf{P}$. The factor $\exp[-iS(\mathbf{P},t,t')]$ then describes the motion of the electron moving between t' and t in the laser field. Finally, the electron recombines at time t with an amplitude equal to $\langle\Phi_i|[i\boldsymbol{\nabla}+e\mathbf{A}_c(t)]|\mathbf{P}\rangle$ and emits a harmonic photon.

IV. DISCUSSION AND CONCLUSION

In the frequency domain, HHG is described as a two-step process. First, a bound electron makes a transition from the ground state to a quantized-field Volkov state under the interaction of the laser field. The electron then returns to the ground state and emits a harmonic photon. Importantly, each stage of the process is physical (i.e., no off-energy-shell entities appear) and can be described by a simple analytical expression. Step-by-step energy conservation is achieved in all subprocesses. We may compare the relative merits of the frequency-domain and time-domain pictures. The time-domain picture investigates the electron trajectories and has the advantage of explaining the cutoff law. In contrast, the frequency-domain picture has the advantage of establishing the connection between HHG and ATI. Moreover, the origin of the plateau is revealed in the frequency-domain picture, i.e., the plateau reflects the characteristics of LAR. Since LAR corresponds to the transitions from the quantized-field Volkov state to the ground state, enormous numbers of electron trajectories will be involved. Finally, there is a strong trend in the literature to regard the dipole momentum $\mathbf{D}(t)$ as a real value [6], i.e., $\mathbf{D}(t)=\mathbf{D}^+(t)+[\mathbf{D}^+(t)]^*$. On the other hand, Kuchiev and Ostrovsky [3] distinguish between the initial and the final states of the HHG process and obtain $\mathbf{D}(t)=\mathbf{D}^+(t)+\mathbf{D}^+(-t)$. They explain the term $\mathbf{D}^+(-t)$ as an unnatural sequence of events, in which emission of high harmonics is followed by absorption of a large number of the laser quanta. In our theory, the underlying physics of $\mathbf{D}^-(t)$ in Eq. (14), derived from the second term in Eq. (5), is clear because energy conservation is guaranteed at all steps.

In our theory, we take a Fock state as the initial state of the light field. Although a coherent state is a more appropriate choice for describing the laser field, it will not affect our results. The reason is the following. A coherent state $|\alpha\rangle$ can be expressed as a coherent superposition of Fock states, i.e., $|\alpha\rangle=\exp(-|\alpha|^2)\Sigma_{n=0}^{\infty}(\alpha^n/\sqrt{n!})|n\rangle$, where $|\alpha|^2$ is the average photon number in the laser field. If we take $|\alpha\rangle$ as the initial state, the amplitude of the qth order harmonic becomes $\exp(-|\alpha|^2)\Sigma_{n=n_0}^{\infty}(\alpha^n/\sqrt{n!})T_n^q$, where T_n^q is the transition matrix element for the qth order harmonic when the initial state is $|n\rangle$. Here, the lower limit of the summation is replaced by a large number n_0 since the probability of finding the coherent state $|\alpha\rangle$ in the n-photon state shows a Poisson distribution with uncertainty equal to the square root of the average photon number; therefore, the contribution to HHG from states with small photon numbers can be neglected. In the large photon number approximation, T_n^q equals $T^{(q)}$, which is dependent on the average photon number of the laser field, while it is independent of the particular initial photon number n [8]. Therefore, whether the initial state is a Fock state or a coherent state will not affect our results. As is well known, a Fock state has definite number of photons while the phase is entirely undetermined. Meanwhile, from the semiclassical description of HHG the time-dependent phase of the classical field is of utmost importance [4]. In our theory the relevant phase is retained in the quantized-field Volkov state. The relation between quantized-field Volkov states and the classical-field Volkov states has been established from the viewpoint of Floquet's theory [8]. In fact, by making a unitary transformation of the quantized-field Volkov state, i.e., $U(t)|\Psi_{\mathbf{P}n}^0\rangle$, the time-dependent phase can be recovered. To derive the Landau-Dykhne formula the Fock states $|n+j\pm1\rangle$ and $|n+j\pm2\rangle$ are replaced by $|n+j\rangle$ when we evaluate the matrix elements $\langle\psi_f|U^{\dagger}(t)V'(t)U(t)|\Psi_{\mathbf{P}n,0}^0\rangle$ and $\langle\Psi_{\mathbf{P}n,0}^0|U^{\dagger}(t')V(t')U(t')|\psi_i\rangle$ in Eq. (12). From the QED viewpoint, however, $|n+j\rangle$, $|n+j\pm1\rangle$, and $|n+j\pm2\rangle$ are different states even though $n\rightarrow\infty$ because $\langle n+j\pm1|n+j\rangle=\langle n+j\pm2|n+j\rangle=0$.

In conclusion, we study the interrelation between HHG and ATI in the frequency domain. HHG can be described simply as ATI followed by LAR. The plateau reflects mainly the characteristics of LAR. We also study the correspondence between frequency-domain and time-domain pictures of HHG.

ACKNOWLEDGMENTS

It is a pleasure to acknowledge stimulating discussions with Professor D. S. Guo. This work was supported by the Chinese Academy of Sciences, the National Natural Science Foundation of China, and the Climbing Program from the Chinese Commission of Science and Technology. B. Wang thanks Professor W. Becker for stimulating discussions.

[1] J. H. Eberly, Q. Su, and J. Javanainen, Phys. Rev. Lett. **62**, 881 (1989).
[2] W. Becker, A. Lohr, M. Kleber, and M. Lewenstein, Phys. Rev. A **56**, 645 (1997).
[3] M. Yu. Kuchiev and V. N. Ostrovsky, Phys. Rev. A **60**, 3111 (1999).
[4] P. B. Corkum, Phys. Rev. Lett. **71**, 1994 (1993).
[5] W. Becker, S. Long, and J. K. McIver, Phys. Rev. A **50**, 1540 (1994).
[6] M. Lewenstein, Ph. Balcou, M. Yu. Ivanov, A. L'Huillier, and P. B. Corkum, Phys. Rev. A **49**, 2117 (1994).
[7] B. W. Shore and P. L. Knight, J. Phys. B **20**, 413 (1987).
[8] L. Gao, X. Li, P. Fu, R. R. Freeman, and D.-S. Guo, Phys. Rev. A **61**, 063407 (2000). Errors have been found in Eq. (19). Corrections will be given elsewhere.
[9] I. Bialynicki-Birula and Z. Bialynicka-Birula, Phys. Rev. A **8**, 3146 (1973), and references therein.
[10] L. W. Keldysh, Zh. Éksp. Teor. Fiz. **47**, 1945 (1964) [Sov. Phys. JETP **20**, 1307 (1965)]; F. H. M. Faisal, J. Phys. B **6**, L89 (1973); H. R. Reiss, Phys. Rev. A **22**, 1786 (1980).
[11] D.-S. Guo and T. Åberg, J. Phys. A **21**, 4577 (1988); D.-S. Guo and G. W. F. Drake, *ibid.* **25**, 3383 (1992).
[12] J. Z. Kaminski and F. Ehlotzky, Phys. Rev. A **54**, 3678 (1996).